

Chapter 4

One-particle transfer

In what follows we present a derivation of the one-particle transfer differential cross section within the framework of the distorted wave Born approximation (DWBA)

(Tobocman (1961), Austern (1963), Satchler (1980); Broglia and Winther (2004), Satchler (1983), Austern (1970), Glendenning, N. K. (2004) and refs. therein.)

The structure input in the calculations are mean field potentials and single-particle states dressed, within the formalism of Nuclear Field Theory, (Bohr, A. and Mottelson, 1975; Bès et al., 1974; Bès and Broglia, 1975; Bès et al., 1976a,b,c; Mottelson, 1976; Broglia et al., 1976; Bès and Broglia, 1977; Bortignon, P. F. et al., 1977; Bès, D. R. and Kurchan, 1990) through the coupling with the variety of collective, (quasi-) bosonic vibrations, leading to modified formfactors¹. With the help of these modified formfactors (Vaagen et al. (1979); Bang et al. (1980); Hamamoto (1970) and refs. therein) and of global optical potentials, one can calculate the absolute differential cross sections, quantities which can be directly compared with the experimental findings.

In this way one avoids to introduce, let alone use spectroscopic factors, quantities which are rather elusive to calculate consistently (Duguet, T. and Hagen (2012); Jenning, B. (2011); Dickhoff and Barbieri (2004); Dickhoff, W. and Van Neck (2005), and refs. therein). This is in keeping with the fact that as a nucleon moves through the nucleus it feels the presence of the other nucleons whose configurations change as time proceeds. It takes time for this information to be feed back on the nucleon. This renders the average potential nonlocal in time (Mahaux, C. et al. (1985) and references therein, cf. also App. 4.I). A time-dependent operator can always be transformed into an energy-dependent operator, implying an ω -dependence of the properties which are usually adscribed to particles like (effective) mass, charge, etc (see App. 4.B). Furthermore, due to (see e.g. App. 1.B)

¹It is of notice that single-particle modified formfactors have their counterpart in the renormalised transition densities (Appendice introduction (inelastic scattering)) and in the modified two-nucleon transfer formfactors (Chapter 5, Eqs. (5.2.48; simultaneous), (5.2.135–5.2.136; successive) and (5.2.155–5.2.156; non-orthogonality) associated with inelastic and with pair transfer reactions (cf. Broglia, R.A. et al. (1973); Potel, G. et al. (2013) and refs. therein), respectively (cf. App. 4.H).

*) See

*****)

253

**) ←

***) Barranco et al (2017) and Sect. 4.2.2;
see also ←

*****)

~~(app. 4.I)~~

Pauli principle, the average potential is also non local in space (cf. App. 4.A). Consequently, one is forced to deal with nucleons which carry around a cloud of (quasi) bosons, aside from exchanging its position with that of the other nucleons, properties which eventually result in a dynamical shell model. It is of notice that the above mentioned phenomena are not only found in nuclear physics, but are universal within the framework of many-body systems as well as of field theories like quantum electrodynamics (QED). In fact, a basic result of such theories is that nothing is really free (Feynman, 1975). A textbook example of this fact is provided by the Lamb shift, resulting from the dressing of the hydrogen's atom electron, as a result of the exchange of this electron with those participating in the spontaneous, virtual excitation (zero point fluctuations (ZPF)) of the QED vacuum (cf. Apps 4.C, 4.D and 4.E). Within this context, in Section 4.2.1 we provide examples of one-particle transfer processes between nuclei lying along the stability valley, populating strongly renormalized quasiparticle states. In Section 4.2.2 (Poner aquí el apendice W) we again take up the subject, but in this case for the exotic, halo nucleus ^{11}Li , in particular in connection with the phenomenon of parity inversion in connection with $N=6$ magic number.

Finally, in Sect. 4.2.3 we discuss the close relation existing, in particular in halo exotic nuclei, between $\beta = 0, \pm 1, \pm 2$ modes. The nucleus ^{11}Li is used as example

^{11}Be

4.1 General derivation

We now proceed to derive the transition amplitude for the reaction (Fig. 4.1.1).

$$A + a (= b + 1) \longrightarrow B (= A + 1) + b. \quad (4.1.1)$$

For a simplified version we refer to App 4.F, while for an alternative derivation within the framework of one-particle knock-out reactions we refer to App 4.G. Let us assume that the nucleon bound initially to the core b is in a single-particle state with orbital and total angular momentum l_i and j_i respectively, and that the nucleon in the final state (bound to core A) is in the l_f, j_f state. The total spin and magnetic quantum numbers of nuclei A, a, B, b are $\{J_A, M_A\}, \{J_a, M_a\}, \{J_B, M_B\}, \{J_b, M_b\}$ respectively. Denoting ξ_A and ξ_b the intrinsic coordinates of the wavefunctions describing the structure of nuclei A and b respectively, and \mathbf{r}_{An} and \mathbf{r}_{bn} the relative coordinates of the transferred nucleon with respect to the CM of nuclei A and b respectively, one can write the "intrinsic" wavefunctions of the colliding nuclei A, a as

$$\phi_{M_A}^{J_A}(\xi_A), \\ \Psi(\xi_b, \mathbf{r}_{b1}) = \sum_{m_i} \langle J_b j_i M_b m_i | J_a M_a \rangle \phi_{M_b}^{J_b}(\xi_b) \psi_{m_i}^{j_i}(\mathbf{r}_{bn}, \sigma), \quad (4.1.2)$$

while the "intrinsic" wavefunctions describing the structure of nuclei B and b are

$$\phi_{M_b}^{J_b}(\xi_b), \\ \Psi(\xi_A, \mathbf{r}_{A1}) = \sum_{m_f} \langle J_A j_f M_A m_f | J_B M_B \rangle \phi_{M_A}^{J_A}(\xi_A) \psi_{m_f}^{j_f}(\mathbf{r}_{An}, \sigma). \quad (4.1.3)$$

*) Feynman 1975

CHAPTER 4. ONE-PARTICLE TRANSFER

For an unpolarized incident beam (sum over M_A, M_a and divide by $(2J_A + 1), (2J_a + 1)$), and assuming that one does not detect the final polarization (sum over M_B, M_b), the differential cross section in the DWBA can be written as

$$\frac{d\sigma}{d\Omega} = \frac{k_f}{k_i} \frac{\mu_i \mu_f}{4\pi^2 \hbar^4} \frac{1}{(2J_A + 1)(2J_a + 1)} \times \sum_{M_A, M_a} \left| \sum_{m_i, m_f} \langle J_b j_i M_b m_i | J_a M_a \rangle \langle J_A j_f M_A m_f | J_B M_B \rangle T_{m_i, m_f} \right|^2, \quad (4.1.4)$$

where k_i and k_f are the relative motion linear momentum in both initial and final channels (flux), while μ_i and μ_f are the corresponding relative masses. The two quantities within $\langle \rangle$ brackets are Clebsch-Gordan coefficients taking care of angular momentum conservation (see Brink and Satchler (1968) and Edmonds (1960), also Bohr and Mottelson (1969)).

The transition amplitude T_{m_i, m_f} is

$$T_{m_i, m_f} = \sum_{\sigma} \int d\mathbf{r}_f d\mathbf{r}_{bn} \chi^{(-)*}(\mathbf{r}_f) \psi_{m_f}^{j_f*}(\mathbf{r}_{An}, \sigma) V(r_{bn}) \psi_{m_i}^{j_i}(\mathbf{r}_{bn}, \sigma) \chi^{(+)}(\mathbf{r}_i), \quad (4.1.5)$$

where

$$\psi_{m_i}^{j_i}(\mathbf{r}_{An}, \sigma) = u_{j_i}(r_{bn}) [Y^{l_i}(\hat{r}_i) \chi(\sigma)]_{j_i m_i}, \quad (4.1.6)$$

is the single-particle wavefunction describing the motion of the nucleon to be transferred, when in the initial state, u, Y and χ being the radial, angular (spherical harmonics) and spin components. Similarly for $\psi_{m_f}^{j_f}$. The distorted waves describing the relative motion of the incoming projectile and of the target nucleus and of the outgoing system and the residual nucleus are,

$$\chi^{(+)}(\mathbf{k}_i, \mathbf{r}_i) = \frac{4\pi}{k_i r_i} \sum_l l'' e^{i\sigma'_i} g_l(\hat{r}_i) [Y^l(\hat{r}_i) Y^l(\hat{k}_i)]_0^0, \quad (4.1.7)$$

and

$$\chi^{(-)*}(\mathbf{k}_f, \mathbf{r}_f) = \frac{4\pi}{k_f r_f} \sum_l l'' e^{i\sigma'_f} f_l(\hat{r}_f) [Y^l(\hat{r}_f) Y^l(\hat{k}_f)]_0^0, \quad (4.1.8)$$

respectively. In the above relations f and g are, respectively, the solutions of the radial Schrödinger equation describing the relative motion associated with the corresponding optical potential ("elastic" scattering) in entrance and exit channel. Let us now discuss the angular components involved in the reaction process, starting with the relation

$$\begin{aligned} [Y^l(\hat{r}_f) Y^l(\hat{k}_f)]_0^0 [Y^l(\hat{r}_i) Y^l(\hat{k}_i)]_0^0 &= \sum_K ((ll)_0 (l'l')_0 | (ll')_K (l'l')_K)_0 \\ &\times \left\{ [Y^l(\hat{r}_f) Y^l(\hat{r}_i)]^K [Y^l(\hat{k}_f) Y^l(\hat{k}_i)]^K \right\}_0^0. \end{aligned} \quad (4.1.9)$$

*)

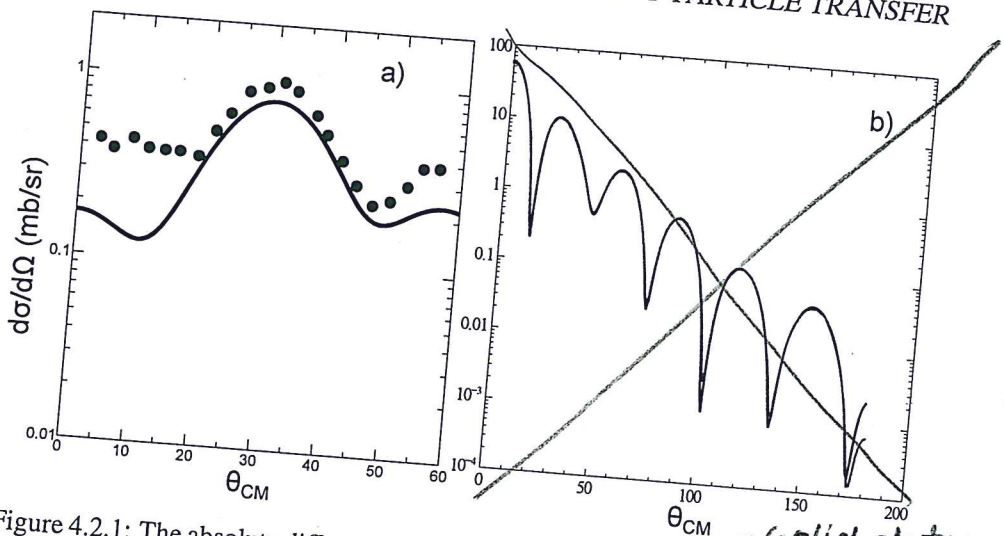


Figure 4.2.1: The absolute differential cross section $^{120}\text{Sn}(p, d)^{119}\text{Sn}(j^\pi)$ associated with the state $j^\pi = 7/2^+$. The theoretical prediction discussed in the text is displayed in comparison with the experimental data (Dickey, S. A. et al. (1982)). The corresponding integrated cross sections are 5.0 and 5.2 ± 0.6 mb respectively. b) Comparison of the results of ONE and of the software FRESCO for the same reaction as in (a) but populating the $5_{1/2}^+$ state.

4.2.1 $^{120}\text{Sn}(p, d)^{119}\text{Sn}$ and $^{120}\text{Sn}(d, p)^{121}\text{Sn}$ reactions.

In the calculation of absolute reaction cross section two elements melt together: reaction and structure. In the case of weakly coupled probes like, as a rule, direct one-particle transfer processes are, the first element can be further divided into two essentially separated components: elastic scattering (optical potentials), and transfer amplitudes connecting entrance and exit channels. In other words, the habitat of DWBA.

In Fig. 4.2.1 (a) a concrete embodiment of the formalism presented in the first part of this Chapter, worked out with the help of the software ONE (Patel, G. (2012)) of global optical parameters (Dickey, S. A. et al. (1982)) and of NFT spectroscopic amplitudes (Table 4.2.1), is given. In it the absolute differential cross section associated with the population of the low-lying state $|^{119}\text{Sn}(5/2^+; 88\text{keV})\rangle$ in the one-particle pick-up process $^{120}\text{Sn}(p, d)^{119}\text{Sn}$ is compared with the experimental data. In Fig. 4.2.1 (b) the theoretical predictions were obtained with the help of ONE.

Similar calculations (ONE, NFT spectroscopic amplitudes and global optical parameters), have been carried for the reaction $^{120}\text{Sn}(d, p)^{121}\text{Sn}(j^\pi; E_x)$ in connection with the population of the $|3/2^+; \text{gs}\rangle$ and $|11/2^-; E_x \approx 0 \text{ MeV}\rangle$ states. In the stripping experiment (Bechara, M. J. and Dietzsch (1975)) the ground state and the $11/2^-$ state were not resolved in energy. This is the reason why theory and experiment are only compared to the data for the summed $l = 2 + 5$ differential cross

*) Patel G. (2012)

**) Dickey, S. A. et al. (1982)

***)

ONE

Software

unpublished

$^{120}\text{Sn}(p, d)^{119}\text{Sn}$	
EXP.	TH
$J^\pi = \frac{3}{2}^-(\frac{3}{2}^+)$	EX (MeV) EX $\bar{\nu}^2$
$\frac{7}{2}^+(\frac{9}{2}^+)$	0.783 0.37 0.66

theoretical effective occupation probability $\bar{\nu}^2$ (Idini et al (2015))

4.2. EXAMPLES AND APPLICATIONS

A. Idini et al., Phys. Rev. C ²⁶³ 031304(R) (2015)

section (cf. Fig. 4.2.2 (a)), the separate theoretical predictions been displayed in Figs. 4.2.2 (b) and (c). (2015)

Let us now turn to the most fragmented low-lying quasiparticle state around ^{120}Sn , namely that associated with the $d_{5/2}$ orbital (cf. Idini, A. (2013), Idini, A. et al. (2012)). As shown in Fig. 4.2.3 five low-lying $5/2^+$ states have been populated in the reaction $^{120}\text{Sn}(p, d)^{119}\text{Sn}$ with a summed cross section $\sum_{i=1}^5 \sigma(2^\circ - 25^\circ) \approx 8 \text{ mb} \pm 2 \text{ mb}$ (Dickey, S. A. et al. (1982)) while four are theoretically predicted with $\sum_{i=1}^4 \sigma(2^\circ - 25^\circ) = 6.2 \text{ mb}$ (cf. also Idini, A. et al. (2014)). Within the present context, namely that of probing the single-particle content of an elementary excitation, the study of the $5/2^+$ quasiparticle strength is a rather trying situation, providing Arguably, it provides a measure of the limitations encountered in such studies.

Analysis of the type presented above allows one to posit that structure and reactions are but just two aspects of the same physics. If one adds to this picture the fact that the optical potential –that is, the energy and momentum dependent nuclear dielectric function describing the medium where direct nuclear chemistry takes place– can be calculated microscopically (cf. Mahaux, C. et al. (1985), Fernández-García, J.P. et al. (2010), Fernández-García, J.P., M. Rodríguez-Gallardo et al. (2010), Broglia, R. A. et al. (1981), Pollaro et al. (1983), Broglia and Winther (2004), Dickhoff, W. and Van Neck (2005), Jenning, B. (2011), Montanari et al. (2014)) in terms of the same elements entering structure calculations (i.e. spectroscopic amplitudes, single-particle wavefunctions, transition densities and eventually effective formfactors), the structure reaction loop closes itself.

Allowing halo nuclei to be part of the daily nuclear structure paradigm, the equivalence between structure and reactions becomes even stronger, in keeping with the central role the continuum plays in the structure of these nuclei.

Searching for further contact points between structure and reactions, one can posit that the above parlance, although being essentially correct, does not emphasize enough the central role virtual, correlated particle-hole excitations play in the single-particle transfer process. In fact, as a result of the interweaving of single-particle (quasiparticle) motion and e.g. collective surface vibrations, particles become dressed, being able to contribute less (differently) to the direct transfer process but, eventually, opening new doorway channels (states) (cf. Feshbach (1958), Rawitscher, G. H. (1987), Bortignon and Broglia (1981), Bertsch et al. (1983)) to depopulate the entrance channel (cf. figura 1D4 de la introducción), similar to those responsible for the breaking of the single-particle strength ($Z_\omega (= m/m_\omega)$) and of the damping of giant resonances and of the renormalization of low-lying collective states (cf. Figs. 4.C.2, 4.C.3, 4.E.1, 4.E.2; cf. also App. 4.I).

It seems then fair to state that the importance of the coupled channels approach to reactions (cf. e.g. Thompson (1988), Thompson, I.J. (2013), Tamura, T. et al. (1970), Ascuutto and Glendenning (1969), Ascuutto, R. J. and Glendenning (1970), Ascuutto R. J. et al. (1971), Ascuutto R.J. and Sørensen (1972); cf. also Fernández-García, J.P. et al. (2010), Fernández-García, J.P., M. Rodríguez-Gallardo et al. (2010)) is not so much, or at least not only, that it is able to handle situations like for example one-particle transfer to members of a rotational band, alas at the

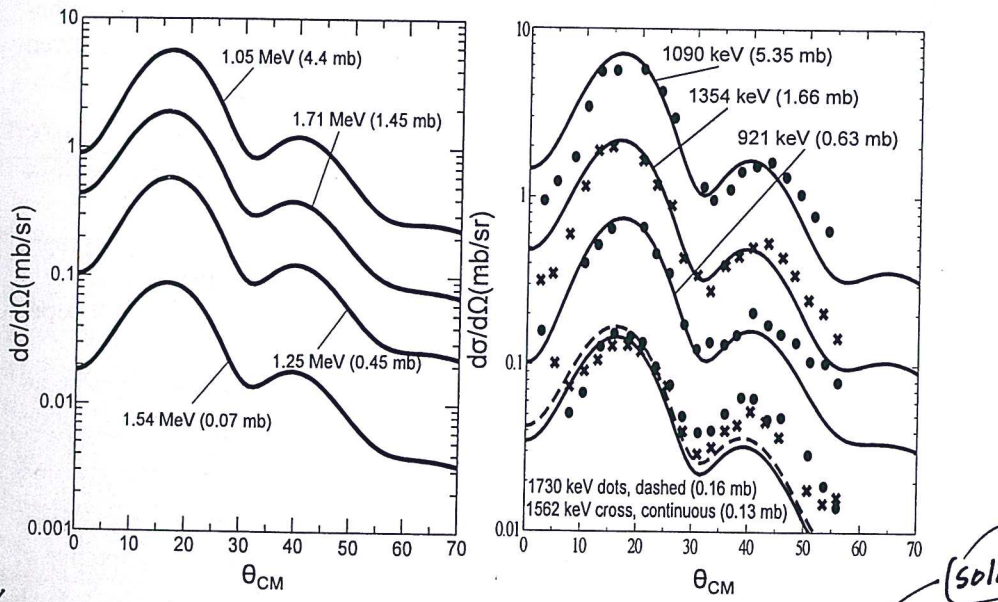
*) Dickey, S. A. et al (1982) ←

**) → gregory, add latest refs.

***) ←

****) ←

For table and caption
see p. 231
version
October 30, 2015
Table 4.2.1



✓ Figure 4.2.3: $^{120}\text{Sn}(p, d)^{119}\text{Sn}(5/2^+)$ absolute experimental cross sections (dots, Dickey, S. A. et al. (1982)), together with the DWBA fit carried out in the analysis of the data (right panel) in comparison with the finite range, full recoil DWBA calculations carried out with global optical potentials making use of NFT structure inputs as explained in the text (after Idini, A. et al. (2014)) and of the software ONE (Potel, G. (2012)); see also App. 6.D.

5

j	E_j (MeV)	$^{120}\text{Sn}(p, d)^{119}\text{Sn}(j)$	$^{120}\text{Sn}(d, p)^{121}\text{Sn}(j)$
$h_{11/2}$	1.54	(1.34) 0.25 (0.28)	(1.25) 0.55 (0.49)
$d_{3/2}$	1.27	(1.27) 0.35 (0.41)	(1.25) 0.41 (0.44)

2 $(E_j, \bar{V}_j^2, \bar{U}_j^2)$ ✓ Table 4.2. The properties of the main peaks of the $h_{11/2}$ and $d_{3/2}$ strength functions of ^{120}Sn calculated taking into account the interweaving of fermionic and bosonic elementary modes of excitation within NFT and of their consequences in both the normal and abnormal densities (cf. Idini, A. et al. (2012); Idini, A. (2013) see also Idini, A. et al. (2014) where the spin degrees of freedom, solely repulsive pairing channel (1S_0) in finite nuclei, has also been included). In parenthesis, experimental (energies) and empirical (single-particle strength) data are given (Bechara, M. J. and Dietzsch (1975), Dickey, S. A. et al. (1982)). (2015)

component
of the

including effects to all orders which can be treated in lowest one expenses of eventually adjusting the optical potential, but that it reminds us how intimately connected probe and probe are in nuclei. with

On the other hand, for most of the situations dealt in the present monograph, it is transparent the power, also to reflect the physics, of the approach based in perturbative DWBA (e.g. 1st order for one-nucleon transfer and 2nd for Cooper pair tunneling), coupled with NFT elementary modes of nuclear excitation.

To which extent a FRESCO like software built on a NFT basis will ever be attempted is an open question. Note in any case the serious attempts made at incorporating so called core excitations within the FRESCO framework (Fernández-García, J.P. et al. (2010), Fernández-García, J.P., M. Rodríguez-Gallardo et al. (2010)).

We conclude this section by recalling the fact that the dressing of single particles with pairing vibrations plays also a central role in the structure properties of nuclei (e.g. Barranco et al. (1987), Bès, D. R. et al. (1988), Baroni, S. et al. (2004) and refs. therein).

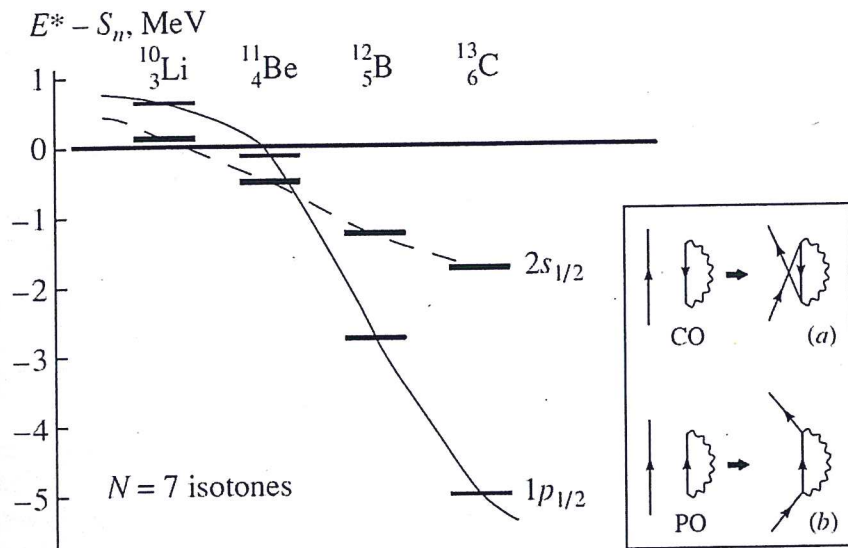
4.2.2 Dressing of single-particle states: parity inversion in ^{11}Li . $4, 2, 2, 3$

The $N = 6$ isotope of ^9Li displays quite ordinary structural properties and can, at first glance, be thought of a two-neutron hole system in the $N = 8$ closed shell. That this is not the case emerges clearly from the fact that ^{10}Li is not bound. In addition, the observation that the two lowest unoccupied states are the virtual ($1/2^+$) and the resonant ($1/2^-$) states, testify to the fact that, in the present case, $N = 6$ is a far better magic neutron number than $N = 8$. In addition, the observation that the unbound $s_{1/2}$ state lies lower than the unbound $p_{1/2}$ state, a phenomenon known in the literature as parity inversion (see Fig. 4.2.4), is in plain contradiction with static mean field theory. Dressing the (standard) mean field (the Saxon-Woods potential, Bohr and Mottelson (1969) Eqs. (2-181)-(2-182)) single-particle states with vibrations of the ^9Li core in terms of polarization (effective mass-like) and correlation (vacuum zero point fluctuations (ZPF)) diagrams, similar to those

4.2.2 NFT of ^{11}Be : one-particle transfer and resonant states.

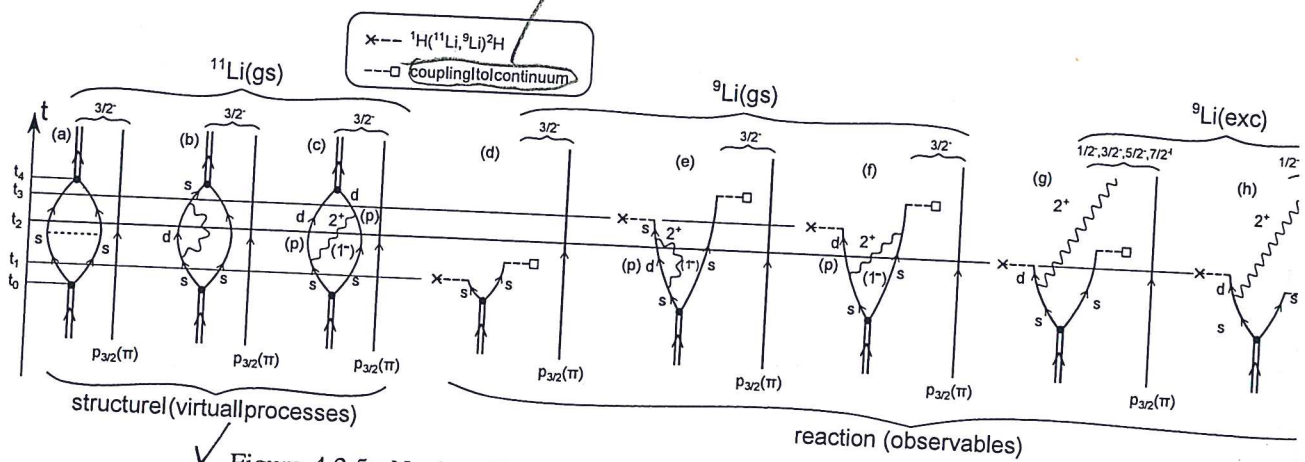
*) \leftarrow **)

* * *) \leftarrow



✓ Figure 4.2.4: Single-particle states for $N = 7$ isotones around ^{11}Be associated with parity inversion. The thin horizontal lines represent the $1p_{1/2}$ single-particle state, while the thick ones the $2s_{1/2}$ orbital. In the case of ^{10}Li one reports the centroid of the virtual and of the resonant states. E^* stands for excitation energy and S_n is the neutron separation energy. In the case of ^{10}Li e.g. $S_n = 0$, while $E_{s_{1/2}}^* = 0.2$ MeV and $E_{p_{1/2}}^* = 0.5$ MeV. In the inset the correlation (CO) and polarization (PO) (virtual) contribution to the single-particle self-energy are shown. An arrowed line pointing upwards represents a particle moving in a level with energy $\epsilon_k > \epsilon_F$, a downwards pointing line represents a hole state $\epsilon_i < \epsilon_F$, while a wavy line stands for a ph-like vibrational state. Their contribution to the real (single-particle "legs" propagating to $\pm\infty$ times) processes dressing the $1p_{1/2}$ and $2s_{1/2}$ neutron states of ^{10}Li and ^{11}Be are (a) and (b), respectively. In the first case the phonon corresponds essentially only to the 2^+ vibration of the corresponding core ^9Li and ^{10}Be , respectively) and pushes the orbital upwards (Pauli principle, Lamb-shift-like process) making the dressed $p_{1/2}$ orbital more strongly unbound than what it was originally in the Saxon-Woods potential. In the case of the $2s_{1/2}$ orbital, it is mainly the process (b) which dresses the state making it almost bound (virtual state) as compared with the Saxon-Woods state. Within this context, it is of notice that in the binding of the two halo neutrons of ^{11}Li to the ^9Li core, it is essentially the pigmy resonance of ^{11}Li which provides the largest contribution, the coupling to the 2^+ vibration of the core ^9Li giving a small shift in energy (nonetheless, it is this weak component of the self energy which is responsible for the excitation, in the $^{11}\text{Li}(p, t)^9\text{Li}$ reaction, of the $1/2$, 2.69 MeV state). In the case of ^{11}Be the (ph) vibrations are the 2^+ , 1, and 3 of the core ^{10}Be , in keeping also with the fact that ^{12}Be does not display a pigmy 1 resonance, not at least based on the ground state. It is of notice that graphs (a) and (b) give rise to an effective mass known as the ω -mass. Associated with it are the $Z(\omega) = (m_\omega/m) - 1$ occupation factors (discontinuity at the Fermi energy).

(in the process (a),)



✓ Figure 4.2.5: Nuclear Field Theory diagrams describing the basic, lowest order processes, by which the di-neutron halo binds to the $^{3}\text{Li}_6$ core to give rise to ^{11}Li ground state (**structure**), and those associated with a one-neutron pick-up process, e.g. $^{1}\text{H}(^{11}\text{Li}, ^{10}\text{Li})^{2}\text{H}$ (**reaction**). The vibrational states of the core ^{9}Li are here represented by the quadrupole mode 2^+ , although in the calculations particle-hole modes with $\lambda^\pi = 3^-, 4^+$ and 5^- were also considered. The state (1^-) associated with the $s \rightarrow (p)$ single-particle states shown in (c) corresponds to the giant dipole resonance of ^{11}Li (see α component in Eq. (6.1.1)). The contribution of this mode to the binding of the Cooper pair is overwhelming (cf. e.g. App. 2.6).

✓ associated with the (lowest order) Lamb shift Feynman diagrams, (cf. App 4.D), shifts the $s_{1/2}$ and $p_{1/2}$ mean field levels around. In particular the $p_{1/2}$ from a bound state ($\approx -1.2\text{ MeV}$) to a resonant state lying at $\approx 0.5\text{ MeV}$ (Pauli principle, vacuum ZPF process), the $s_{1/2}$ being lowered and becoming a virtual state ($\approx 0.2\text{ MeV}$) (cf. Fig. 2.6.3 (1F3) cf. also Barranco, E. et al. (2001)). While ^{10}Li is not bound, adding a second dressed neutron and allowing them to exchange density vibrations of the core, as well as the pigmy giant resonance resulting from the sloshing back and forth of the outer neutrons as well as those of ^{9}Li against the protons (cf. Appendix 1F y App. 6.A) binds the Cooper pair to ^{9}Li . In fact $^{11}\text{Li}_8$ displays a two-neutron separation energy $S_{2n} \approx 400\text{ keV}$, (for further details we refer to Ch. 6, Sect. 6.1).

→ (II) a) and b) attempt at describing the becoming of the neutron halo Cooper pair of ^{11}Li , from an uncorrelated $s_{1/2}^2(0)$ configuration to a correlated, (weakly) bound two-neutron state. It is of notice that the bare interaction (boxed inset in (II)), lowers the $s_{1/2}^2(0)$ as well as the $p_{1/2}^2(0)$ pure configurations by only 100 keV, and thus it is not able, by itself, to bind the pair, nor to give rise to any significant mixing between these two configurations. The surfaces display the modulus square of the two-neutron wavefunction as a function of the coordinates of the two nucleons (left) and the probability distribution of one neutron with respect to the second one held fixed on the x-axis (at a radius of 5fm, solid dot). The red circle schematically

*) Barranco et al (2001)

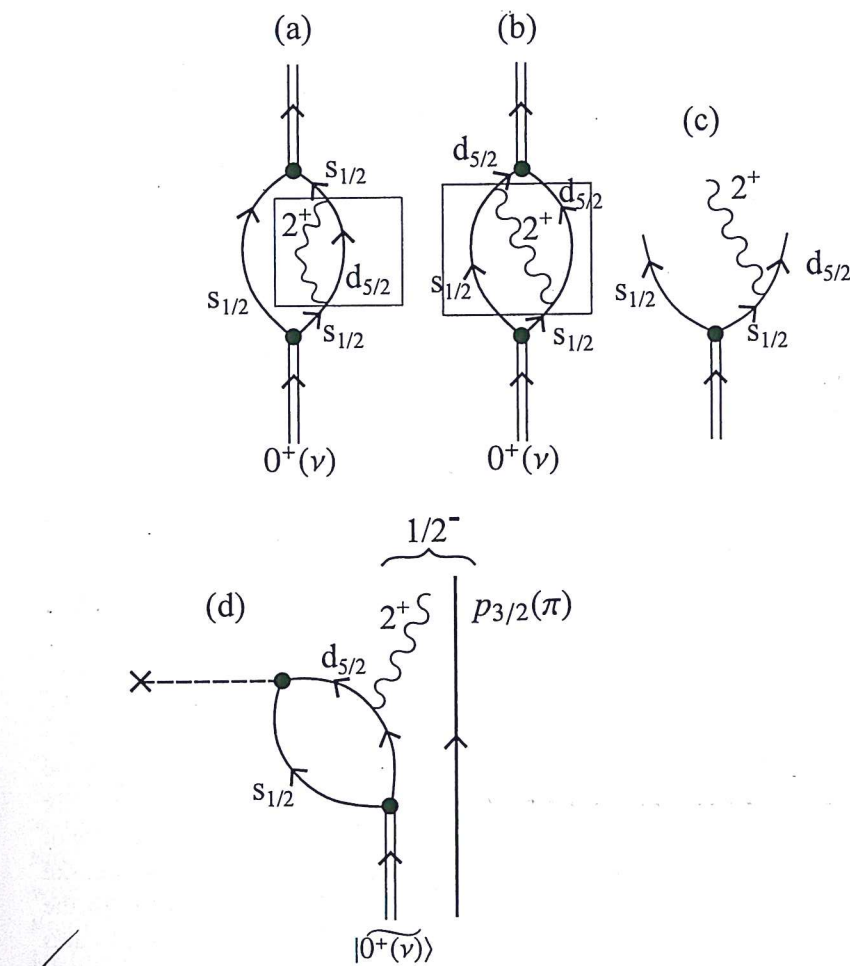


Figure 4.2.6: (a) Self-energy (see boxed process) and (b) vertex (pairing induced interaction) renormalization processes, both diagrams associated with (c) a (two-particle)-(quadrupole vibration) intermediate (virtual state) which can be forced to become real in a (p, t) reaction like e.g. ${}^1\text{H}({}^{11}\text{Li}, {}^9\text{Li}){}^3\text{H}$ exciting the first excited state $|2.69\text{MeV}; 1/2^-\rangle$ of ${}^9\text{Li}$, (see Ch. 6).

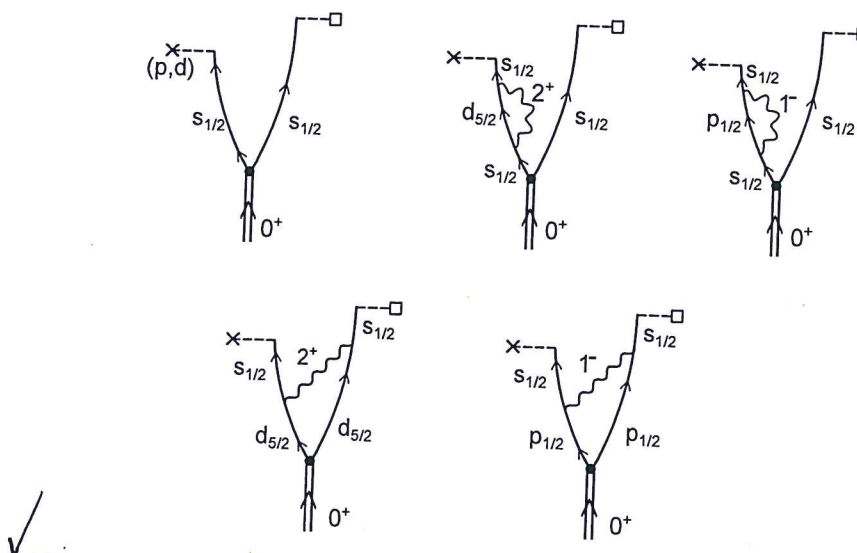


Figure 4.2.7: Lowest order, NFT contributions, to the population of the $s_{1/2}$ lowest resonant ${}^{10}\text{Li}(1/2^+)$ through the pick-up reaction ${}^1\text{H}({}^{11}\text{Li}, {}^{10}\text{Li}(1/2^+)) {}^2\text{H}$. Concerning the notation cf. Caption to Fig. 4.2.5.

represents the core.

How can one check that CO and PO like processes as the ones shown in Fig. 2.6.3 (I) (cf. also Fig. 4.B.1) are the basic processes dressing the odd neutron of ${}^{10}\text{Li}$, and thus the mechanism at the basis of parity inversion? The answer is, forcing these virtual processes to become real. In other words, act on the system with an external field so that certain off-the-energy shell states become on-the-energy shell. In fact, a reaction like ${}^1\text{H}({}^{11}\text{Li}, {}^{10}\text{Li}) {}^2\text{H}$ can populate single-particle states in ${}^{10}\text{Li}$ (see Fig. 4.2.5), in particular the two lowest states of ${}^{10}\text{Li}$, namely the virtual and the resonant $|s_{1/2}\rangle$ and $|p_{1/2}\rangle$ states respectively. The same can be of course done through the reaction ${}^2\text{H}({}^9\text{Li}, {}^{10}\text{Li}) {}^1\text{H}$ (see Orrigo, S. E. A. and Lenske (2009) and Jeppesen, H. B. et al. (2004)). Being these states embedded in the continuum the system will eventually decay into both the ground and excited states of ${}^9\text{Li}$ (cf. Fig. 4.2.5) (referir al apendice W).

Now, indirect information on this questions can also be obtained with the help of two-particle transfer processes, namely that associated with inverse kinematics (p, t) reaction ${}^1\text{H}({}^{11}\text{Li}, {}^9\text{Li}(2.69\text{MeV}; 1/2^-)) {}^3\text{H}$ (Tanihata, I. et al., 2008) populating the first excited state of ${}^9\text{Li}$, thought to be the lowest member of the multiplet $2^+ \otimes p_{3/2}(\pi)$ (cf. Figs. 6.1.1–6.1.3 and 4.2.6). A price to pay for not using the specific probe for single-particle modes (one-particle transfer), is that of adding to the self-energy contributions in question those corresponding to vertex corrections (for details cf. App 4.E, Figs 4.E.1 and 4.E.2 and Ch. 6).

Within the present context, it is difficult if not impossible to talk about single-particle motion without also referring to collective vibrational states (cf. e.g. Fig.

- *) Orrigo S.E.A. and Lenske (2009),
Jeppesen H. B. et al (2004).
- **) Tanihata I. et al., 2008

App. W

RAB

Appendix W

9/8/14 17:01

2.6.3 (II)), or to talk about pair addition and pair subtraction modes, without at the same time talking about correlated particle-hole (e.g. density) vibrations and dressed quasiparticle motion (see e.g. Fig. 4.2.6 (a) and (b)), again concerning both structure and reactions. Within the framework of the present monograph, the above facts imply that Chapters 1, in particular App. ?? 1E, Chapters 4 (one-particle transfer), 5, and 6 (two-particle transfer and applications), form a higher unity. This unity extends also to the content of App 4.G (knock-out reactions), as well as to the question of inelastic channels and of final state interactions, and thus of the possibility that the population of the excited state $1/2^-$ receives contributions other, and more involved, than those associated with the direct two-nucleon pick-up process depicted in Figs. 4.2.5/(g) and (h) and 4.2.6 (d) (for details cf. Ch. 6, in particular App. 6.B, Table 6.B.1) cf. also (Potel et al., 2010)).

Let us now return to the discussion of the one-particle transfer process $^1\text{H}(^{11}\text{Li}, ^{10}\text{Li})^2\text{H}$, that is the pickup of a neutron from the pair addition halo state $|^{11}\text{Li}(\text{gs})\rangle$ (cf. Fig. 4.2.5). In keeping with the fact that ^{10}Li is not bound, such a reaction populates only transiently the virtual and resonant states of ^{10}Li and eventually, after the second neutron of the pair spoliated of its dynamical glue leaves the system by decaying into the continuum, a state in ^9Li is populated (cf. Figs. 4.2.5 (d)-(f) and (g) and (h)). In drawing the different NFT diagrams time t is assumed to run upwards. External fields and the bare NN -interaction are assumed to act instantaneously, while the couplings to the phonon modes (wavy lines) lead to retarded (ω -dependent) effects. For simplicity, only the quadrupole vibrational mode of the ^8He core is considered, as well as only the virtual s - and continuum d - single-particle states are taken into account. The halo Cooper pair (pair addition mode of the $N = 6$ closed shell system) carries angular momentum 0^+ and is represented by a double arrowed line, the odd proton (π) which occupies a $p_{3/2}$ state, is represented by a single arrowed line and is here treated as a spectator. The di-neutron system binds to the core through (a) the bare interaction (horizontal dashed line) acting between the two-neutron, each represented by a single arrowed line, and through the renormalizing processes associated with the coupling of the neutrons with vibrations; (b) effective mass processes associated with the quadrupole vibration of ^9Li (wavy line) renormalizing the energy of the $s_{1/2}$ continuum state and leading to an almost bound (virtual) state (≈ 0.2 MeV) as well as of the p -state and giving rise to a resonant state (≈ 0.5 MeV). (c) Vertex correction (induced pairing interaction) associated with the quadrupole vibration of ^9Li and with the giant dipole pigmy resonance of ^{11}Li . While the quadrupole vibration is essential for parity inversion (single-particle renormalization effect) it plays little role regarding vertex corrections (induced pairing interaction), the pigmy resonance of ^{11}Li plays a central role in binding the Cooper pair, as testified by components $\beta (= 0.1)$ and $\alpha (= 0.7)$ of $|^{11}\text{Li}(\text{gs})\rangle$ (cf. eq. (6.1.1)). Of course, the pigmy resonance plays no role in parity inversion in ^{10}Li , being an excitation of ^{11}Li , nucleus in which it plays little role in the virtual effective mass process of the $s_{1/2}$ and $p_{1/2}$ states of $|0_\nu\rangle$. Picking up a neutron from the halo pair addition mode of ^9Li (that is $|^{11}\text{Li}(\text{gs})\rangle$), it obliterates its symbiotic pigmy resonant state. This is a peculiar

*) Potel et al (2010)

CHAPTER 4. ONE-PARTICLE TRANSFER

example of the fact that not all virtual states can be forced to become real even with the proper external field. On the other hand, the absolute cross section associated with the reaction $^1\text{H}(^{11}\text{Li}, ^{10}\text{Li}(1/2^+))^2\text{H}$ will depend on the variety of renormalization processes displayed in Fig. 4.2.7 (d). Intervening the process (a) at any time after t_0 and before t_4 with an external single-neutron pick-up field (cross followed by an horizontal dashed line), and processes (b) and (c) at $t_0 < t < t_1$, leads to the ground state of ^9Li , in keeping with the fact that the second neutron will leave the system almost immediately, ^{10}Li not being stable. (e) Same as above but in connection with process (b) and now after the nucleon has reabsorbed the quadrupole phonon and before t_4 , i.e. acting at $t_3 < t < t_4$ leads again to the population of the ^9Li ground state. (f) same as (e) but in this case the external field acts on the process (c). Let us now consider the one-nucleon pickup processes populating the $(2 \otimes p_{3/2}(\pi))_{J^\pi}$, ($J^\pi = 1/2^-, 3/2^-, 5/2^-$ and $7/2^-$) multiplet of ^9Li , in particular the lowest $|1/2^-; 2.69 \text{ MeV}$ state. In this case the external field has to act at a time t_2 on (b) and on (c) leading to identical final states displayed in (g) and on (h). While the single contribution associated with mass renormalization process ((b) \rightarrow (g)) and vertex corrections ((c) \rightarrow (h)) cannot be distinguished experimentally, one can estimate the relative contribution to the corresponding absolute cross section making use of microscopic wavefunctions (cf. e.g. Barranco, F. et al. (2001)).

(Born, 1926)

Before concluding the present section, and in connection with Figs. 4.2.7 (g,h) and 4.2.6 (d), it may be useful to remind us what, within the framework of quantum mechanics, one can learn from a reaction experiment. It is not "what is the state after the collision" but "how probable is a given effect of the collision". Within this context: "The motion of particles follows probability laws, but the probability itself propagates according to the laws of causality" (Born, 1926).

(Born, 1926)

If there is a lesson to be learned from the above discussion is the fact that, in dealing with a specific feature of a quantal many-body system, e.g. single-particle motion in nuclei (structure) and one-particle transfer process (reaction), one can hardly avoid to talk about other elementary modes of excitation and reaction channels, respectively. Within the scenario of the chosen example, this is because a nucleon which, in first approximation is in a mean field stationary state, can actually be viewed as a fermion moving through a gas of ephemeral $2p - 2h$ composite virtual excitations, that is $(p-h) +$ density and/or $2h(2p) +$ pair addition (subtraction) modes, arising from vacuum (ground state) ZPF and giving rise to the nuclear vacuum (ω -dependent dielectric function). Because of Pauli principle (Pauli, 1947) the nucleon in question is forced to exchange role with the virtual, off-the-energy-shell nucleons, thus leading to CO processes (Fig. 4.B.1 (b)) and eventually, through time ordering, to PO ones (Fig. 4.B.1 (a)). Such processes, eventually carried to higher orders of perturbation in the nucleon-vibration coupling, diagonalize the nuclear Hamiltonian, taking care of the overcompleteness (non-orthogonality) and of Pauli violations of the basis made out of elementary modes of nuclear excitation, thus leading to dressed (observable) modes, single-particle states in the present case, whose properties, e.g. absolute single-particle transfer cross sections, can be compared with the data without further ado.

*) Barranco et al (2001)